Evaluation of Pharmacokinetics of 4-Borono-2-^{18}F-Fluoro-L-Phenylalanine for Boron Neutron Capture Therapy in a Glioma-Bearing Rat Model with Hyperosmolar Blood–Brain Barrier Disruption

Chia-Hung Hsieh, MS[1]; Yu-Fang Chen, MS[2]; Fu-Du Chen, PhD[1,3]; Jeng-Jong Hwang, PhD[1]; Jyh-Cheng Chen, PhD[1]; Ren-Shen Liu, MD[4]; Ji-Jung Kai, PhD[5]; Chi-Wei Chang, MS[1]; and Hsin-Ell Wang, PhD[1]

[1]Institute of Radiological Sciences, National Yang-Ming University, Taipei, Taiwan; [2]Department of Pharmacy, Taipei Veterans General Hospital, Taipei, Taiwan; [3]Institute of Radiological Sciences, Central Taiwan University of Science and Technology, Taichung, Taiwan; [4]Deprtment of Medicine, National Yang-Ming University, Taipei, Taiwan; and [5]Department of Engineering and System Science, National Tsing Hua University, Hsinchu, Taiwan

This study evaluated the pharmacokinetics and biodistribution of 4-borono-2-^{18}F-fluoro-L-phenylalanine (^{18}F-FBPA) after intracarotid injection and with blood–brain barrier disruption (BBB-D) in F98 glioma-bearing F344 rats. The pharmacokinetics of L-*p*-boronophenylalanine (BPA) and ^{18}F-FBPA following different administration routes were compared to demonstrate the optimal delivery route and the time period for thermal neutron irradiation. **Methods:** F98 glioma-bearing rats were injected intravenously or intracarotidly with ^{18}F-FBPA and BPA and with or without mannitol-induced hyperosmotic BBB-D. The boron concentration and ^{18}F radioactivity in tissues were determined by invasive (inductively coupled plasma mass spectroscopy, γ-counting) and noninvasive PET methods. **Results:** The biodistributions of ^{18}F-FBPA and BPA in F98 glioma-bearing rats were similar after intracarotid administration with BBB-D. The accumulation of BPA and ^{18}F-FBPA in brain tumor and the tumor-to-ipsilateral brain ratios were the highest after intracarotid injection with BBB-D, whereas the retention of boron drugs in contralateral brains exhibited only nonsignificant differences compared with those after intracarotid injection without BBB-D and intravenous injection. The high boron concentration in brain tumor (76.6 μg/g) and the high tumor-to-ipsilateral brain ratio (6.3) may afford enough radiation doses to destroy the tumor cells while sparing the normal tissues in boron neutron capture therapy. The pharmacokinetic parameters of k_{el}, k_{12}, k_{21}, and V_1 for intracarotid injection of ^{18}F-FBPA with BBB-D derived from the open 2-compartment model are 0.0206 ± 0.0018 min^{-1}, 0.0260 ± 0.0016 min^{-1}, 0.0039 ± 0.0003 min^{-1}, and 3.1 ± 0.1 mL, respectively. The effect of BBB-D varied depending on the anesthetic agents used and the anesthetic conditions. A smaller degree of BBB-D and, thus, lower boron concentrations in tumor and ipsilateral brain were observed under isoflurane anesthesia than under ketamine anesthesia. The k_{12}/k_{21} ratio may serve as a good indication for evaluating the extent of BBB-D, tumor uptake, and tumor-to-brain ratio after intracarotid injection of boron compounds. **Conclusion:** Our findings provide important information for establishing an optimal treatment protocol when intracarotid injection with BPA after BBB-D is applied in clinical boron neutron capture therapy.

Key Words: boron neutron capture therapy; 4-borono-2-^{18}F-fluoro-L-phenylalanine; F98 glioma; blood–brain barrier disruption; PET

J Nucl Med 2005; 46:1858–1865

Boron neutron capture therapy (BNCT) is based on the nuclear capture reaction that occurs when ^{10}B is irradiated with thermal or epithermal neutrons to produce high linear energy transfer α-particles and recoiling ^{7}Li nuclei (*1,2*). For successful clinical applications of BNCT, there must be a selective accumulation of ^{10}B in the tumor, low levels in normal tissues, and sufficient thermal neutron fluence delivered to the tumor site. Considerable efforts have been dedicated to the development of boron-delivering agents that could target tumors for BNCT, but, until now, only 2 low-molecular-weight boron compounds, sodium sulfhydryl borane ($Na_2B_{12}H_{11}SH$ [BSH]) and L-*p*-dihydroxyborylphenylalanine (BPA), have been clinically used as neutron capture agents for the treatment of brain tumor and other tumor types (*3,4*). Although these compounds lack specificity, they may attain higher concentrations in neoplastic cells by virtue of a partial compromise of the integrity of the blood–brain barrier (BBB) within the tumor.

Barth et al. (*5,6*) has reported that using intracarotid infusion of a hyperosmotic solution of mannitol, which disrupts the BBB, followed by intracarotid injection of either BPA or BSH, the boron uptake in brain tumor and animal survival could be higher than by other delivery routes. However, the boron content in tumor, normal brain,

Received Dec. 27, 2005; revision accepted Aug. 4, 2005.

For correspondence or reprints contact: Hsin-Ell Wang, PhD, Institute of Radiological Sciences, National Yang-Ming University. 155, Li-Nong St., Section 2, Peitou, Taipei, Taiwan.

E-mail: hewang@ym.edu.tw

and blood after intracarotid injection with BBB disruption (BBB-D) of boron compounds also exhibited higher variation than by other delivery routes. To ensure the efficacy of BNCT, it would be essential to determine the pharmacokinetics and the concentration of boron compounds in brain after intracarotid injection with BBB-D for each individual patient before neutron irradiation is conducted. We used 4-borono-2-^{18}F-fluoro-L-phenylalanine (^{18}F-FBPA) as a PET probe to investigate noninvasively the pharmacokinetics of BPA after hyperosmotic BBB-D in F98 glioma-bearing Fischer 344 rats. The radioactivity of ^{18}F-FBPA in tumor and normal tissues was measured by γ-scintillation counter, and the boron content in tissue samples was determined using inductively coupled plasma mass spectroscopy (ICP-MS). This study demonstrated the pharmacokinetics and biodistribution of ^{18}F-FBPA and BPA after intracarotid injection with hyperosmotic BBB-D in a glioma-bearing rat model. Our results could help in optimizing the treatment protocol for BNCT of brain tumors.

MATERIALS AND METHODS

^{18}F-FBPA Synthesis and F98 Glioma Brain Tumor Model in Rats

The procedures for ^{18}F-FBPA preparation, F98 glioma cell culture, and the glioma-bearing Fischer 344 rat (male, 12–14 wk old, about 250–280 g) model were detailed in our previous report (*7*). The radiochemical purity of ^{18}F-FBPA was >97%. The animal experiments were approved by the Laboratory Animal Care Panel of the National Yang Ming University.

Intracarotid Artery Injection and Osmotic BBB-D

Thirteen days after tumor implantation, the rats were anesthetized by intraperitoneal administration of a 4:1 mixture of ketamine and xylazine at a dose of 0.016 mL/g of body weight (BW) or with isoflurane using a vaporizer system (Fluosorber; VetClick). The left common, external, and internal carotid arteries were exposed, and the proximal portion of the external carotid artery was temporarily clamped with an aneurysm clip. The distal end of a polyethylene (PE 10) catheter linked with a Mini-port (Smiths Medical MD) was inserted into the left external carotid artery, then to the common carotid artery bifurcation, and fixed at the 3- to 4-mm proximal portion of the external carotid artery with an aneurysm clip. The distal portion of the external carotid artery and every branch of the external carotid artery were coagulated, and a small volume of heparin (100 IU/mL of normal saline, <0.4 mL) was infused to ensure that it flowed up the internal carotid artery. After intracarotid injection, the cannula was removed, the external carotid artery was ligated, and the neck dissection was closed. BBB-D was accomplished using the method described by Neuwelt et al. (*8,9*) with some modifications. Briefly, a 25% mannitol solution (1.6 mol/L) was warmed to 37°C, filtered through a 0.22-μm membrane filter (Millex-GV, no. SLGVR25LS; Millipore Corp.), and infused through the catheter into the external carotid artery for 30 s at a rate of 0.25 $mL \cdot kg^{-1} \cdot s^{-1}$. This dose has been reported to produce a reversible BBB-D without significant neuronal damage (*10*). The control animals were infused with normal saline instead of mannitol.

Pharmacokinetics of ^{18}F-FBPA Determined by PET

The procedures for PET were described in detail in our previous report (*7*). PET was performed on the 13th day after tumor implantation. Three groups of rats—intravenous ($n = 3$), intracarotid ($n = 6$), and intracarotid with BBB-D ($n = 6$)—were anesthetized with isoflurane using a vaporizer system and received intracarotid or intravenous injections of ^{18}F-FBPA at a dose of 29.6 MBq/kg of BW for 5 min immediately after intracarotid infusion of either 25% (w/v) mannitol or normal saline. Data acquisition by PET was initiated at the first minute after drug administration. Dynamic coronal images were acquired using ten 60-s frames and ten 2-min frames, followed by 10-min frames up to 4 h after injection. Time–activity curves were plotted for both tumor and ipsilateral normal brain ROIs.

Biodistribution of ^{18}F-FBPA

The biodistribution of ^{18}F-FBPA was determined on the 13th day after tumor implantation. Each tumor-bearing rat was anesthetized with isoflurane using a vaporizer system and received an intracarotid injection of ^{18}F-FBPA at a dose of 29.6 MBq/kg of BW for 5 min immediately after intracarotid infusion of 25% (w/v) mannitol. At 0.5, 2.5, and 4 h after injection, rats were sacrificed with chloroform (Merck, catalog no. 1.02445). Tumors, ipsilateral brain, contralateral brain, and blood were removed, and parts of these tissues were assayed for radioactivity with a γ-scintillation counter (Cobra II Autogamma; Packard). The uptake of ^{18}F-FBPA in tissues was expressed in counts per minute (cpm) corrected with decay and normalized to the percentage injected dose per gram of tissue (%ID/g).

Pharmacokinetic Model Analysis

Blood samples (0.1 mL each) were collected from the femoral arterial catheter during PET at 1, 5, 10, 15, 20, 25, 30, 50, 70, 90, 120, 150, 180, 210, and 240 min after ^{18}F-FBPA administration. The radioactivity of blood samples was assayed with a γ-scintillation counter and was expressed in MBq/mL of blood sample. Pharmacokinetic parameters were estimated after fitting a nonlinear regression curve to the data point of blood radioactivity using the open 2-compartment model ($Cp = Ae^{-\alpha t} + Be^{-\beta t}$). Nonlinear regression analysis using programs incorporating the SigmaPlot software was then performed to calculate the gross rate constants (A, α, B, β). The micro rate constants of k_{el} (rate constant of elimination), k_{12} (rate constant of central compartment to peripheral compartment), k_{21} (rate constant of peripheral compartment to central compartment), and V_1 (central compartment volume of distribution) were calculated using Matlab 6.5 with in-house–designed Matlab codes under Windows XP professional OS.

Biodistribution of ^{10}B-BPA

The biodistribution study of BPA was performed on the 13th day after tumor implantation. Each tumor-bearing rat was anesthetized by intraperitoneal administration of a 4:1 mixture of ketamine and xylazine at a dose of 0.016 mL/g of BW and received intracarotid injection of BPA at a dose of 300 mg/kg of BW for 5 min immediately after intracarotid infusion of 25% (w/v) mannitol. At 0.5, 1, 2, 3, 4, and 6 h after injection, rats were sacrificed with chloroform. Tumor, ipsilateral brain, contralateral brain, and blood were removed and parts of these tissues were assayed for boron concentration by ICP-MS and were calibrated with the standard curve derived from the measurement of boric acid standard (purchased from the National Institute of Standards and Technology). The results were normalized to μg/g of tissue. The advantages of

ICP-MS over other methods are higher sensitivity, lower detection limit, and simultaneous measurement of ^{10}B-to-^{11}B isotopic ratio and total boron content in a sample (*11*).

Effect of Anesthesia on Biodistribution of BPA

The F98 glioma-bearing rats were randomly divided into 2 groups. Group 1 ($n = 6$) rats were each injected intravenously with 500 mg/kg of BW of BPA for 5 min immediately after intracarotid infusion of 25% (w/v) mannitol and kept anesthetized with isoflurane for 2.5 h. Group 2 ($n = 6$) rats received the same drug treatment as in group 1 except that a ketamine mixture was used instead. At 2.5 h after drug administration, rats were sacrificed with chloroform. Tumor, ipsilateral brain, contralateral brain, and blood samples were removed and assayed for boron concentration by ICP-MS. The boron concentration was normalized to μg/g of tissue.

Statistical Analysis

All values are shown as mean ± SD. Statistical analyses were performed using an unpaired Student *t* test to evaluate the significance of differences in values between 2 treated groups. Simple regression analysis was performed to establish the correlation among the radioactivity of tumor ROI, k_{12}/k_{21}, and tumor-to-ipsilateral brain ratio. A 2-tailed value of $P < 0.05$ was considered significant.

RESULTS

Pharmacokinetics of ^{18}F-FBPA Determined by PET

The time–activity curves of ^{18}F-FBPA in tumor and ipsilateral brain derived from dynamic PET images are shown in Figure 1A. The uptake of ^{18}F-FBPA in tumor differed significantly for various delivery routes. Among them, the intracarotid injection with BBB-D was the highest. In contrast to tumor uptake, insignificant differences were found in normal brain uptake of ^{18}F-FBPA in spite of the different administration protocols used. The derived tumor-to-ipsilateral brain ratios after ^{18}F-FBPA administration (Fig. 1B) showed that the ratios were about 5.1 at 145–165 min after intracarotid injection with BBB-D, 3.1 at 98–112 min after intracarotid injection without BBB-D, and 2.4 at 45–62 min after intravenous injection, respectively.

Pharmacokinetic Model Analysis

The time–activity curves of ^{18}F-FBPA in blood after intracarotid injection of ^{18}F-FBPA with and without BBB-D were shown in Figure 2. Biexponential time–activity curves of blood after intracarotid injection of ^{18}F-FBPA with and without BBB-D were observed and, thus, the open 2-compartment model was used to estimate the pharmacokinetic parameters. The pharmacokinetic parameters of k_{el}, k_{12}, k_{21}, and V_1 for intracarotid injection with BBB-D derived from the time–activity curve of ^{18}F-FBPA in blood were 0.0206 ± 0.0018 min^{-1}, 0.0260 ± 0.0016 min^{-1}, 0.0039 ± 0.0003 min^{-1}, and 3.1 ± 0.1 mL, whereas those for intracarotid injection without BBB-D were 0.0071 ± 0.0014 min^{-1}, 0.0160 ± 0.0017 min^{-1}, 0.0061 ± 0.0004 min^{-1}, and 3.6 ± 0.1 mL, respectively (Table 1).

Biodistribution of ^{18}F-FBPA

The accumulation of ^{18}F-FBPA in tumor, ipsilateral brain, contralateral brain, and blood of F98 glioma-bearing Fischer 344 rats at 0.5, 2.5, and 4 h after administration of ^{18}F-FBPA (29.6 MBq/kg of BW) by various routes are shown in Table 2. The biodistribution revealed that the

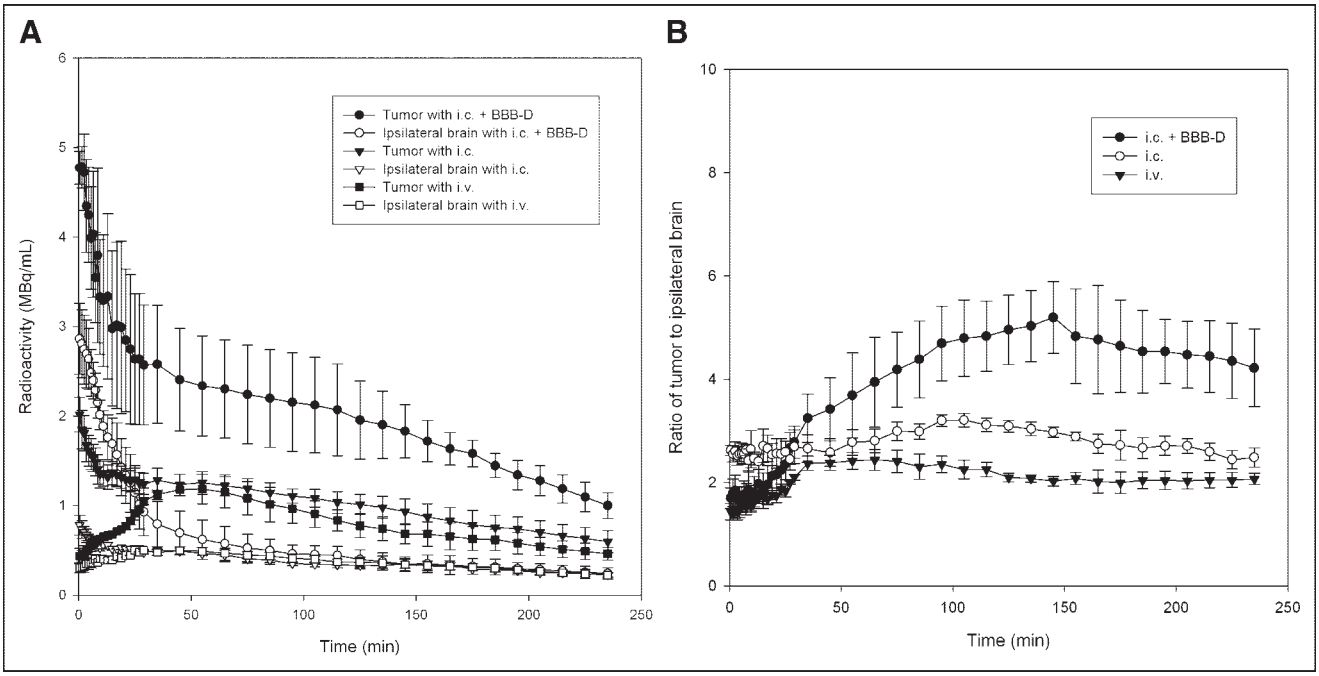

FIGURE 1. Pharmacokinetics of ^{18}F-FBPA for F98 glioma-bearing rats determined by PET. (A) Time–activity curves of ^{18}F-FBPA in tumors and ipsilateral brains of F98 glioma-bearing rats derived from dynamic PET images after intracarotid (i.c.) injection with and without BBB-D and after intravenous (i.v.) injection. (B) Tumor-to-ipsilateral brain ratio of ^{18}F-FBPA.

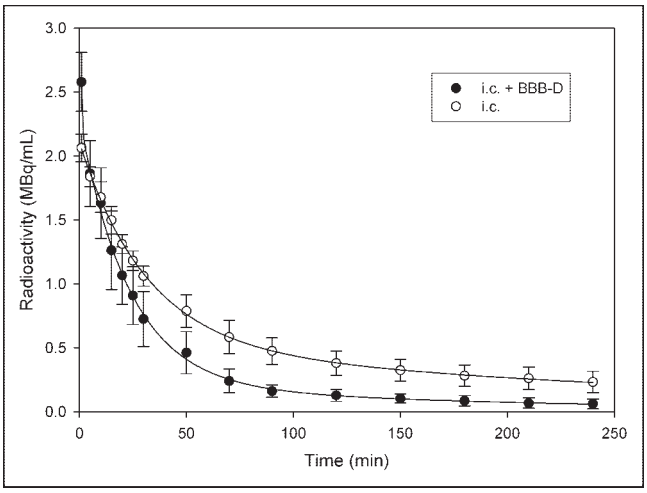

FIGURE 2. Time–activity curves of ^{18}F-FBPA in blood of F98 glioma-bearing Fischer 344 rats after intracarotid (i.c.) injection with and without BBB-D. Data points were fitted with open 2-compartment model ($Cp = Ae^{-\alpha t} + Be^{-\beta t}$). $r^2 = 0.97–0.99$.

uptake of ^{18}F-FBPA in tumor was significantly higher than that in blood and in normal brain during the entire study period. The tumor-to-ipsilateral brain ratio reached a maximum (4.8) at 2.5 h after administration of ^{18}F-FBPA with BBB-D, which confirmed the PET finding (Fig. 1B). Although the tumor-to-contralateral brain and tumor-to-blood ratios were even higher at 4 h (5.9 and 7.9, respectively) than those at 2.5 h (5.7 and 6.7, respectively) after injection, the tumor retention of ^{18}F-FBPA at 4 h (1.48 ± 0.25 %ID/g) was significantly decreased from that at 2.5 h (2.63 ± 0.72 %ID/g).

Biodistribution of ^{10}B-BPA

The boron concentrations in tumor, ipsilateral brain, contralateral brain, and blood at various time after intracarotid injection of 300 mg/kg of BW of BPA with BBB-D were assayed by ICP-MS (Fig. 3A). The time period between 0.5 and 6 h after administration of BPA with BBB-D was taken as the elimination phase. One hour after administration of BPA, the contralateral brain boron concentration–time profile was taken as the absorption phase. The tumor-to-contralateral brain ratio showed a rapid decrease in the first 1 h after drug administration and declined slowly in the elimination phase (Fig. 3B). The tumor-to-ipsilateral brain ratio reached a plateau at 2–3 h after drug administration and then declined slowly. The distribution of boron in F98 glioma-bearing rats at 2.5 h after various routes of administration of 500 mg/kg of BW of BPA is shown in Table 3. The boron concentration in tumor (76.6 ± 12.1 μg/g) was higher after intracarotid injection with BBB-D than that after intracarotid injection without BBB-D (43.1 ± 5.6 μg/g) and after intravenous injection (19.5 ± 4.5 μg/g). Besides, the tumor-to-ipsilateral brain, tumor-to-contralateral brain, and tumor-to-blood ratios were also significantly higher after intracarotid injection with BBB-D than those after intracarotid injection without BBB-D and after intravenous injection (Table 3). The results revealed that the intracarotid injection with BBB-D would be the optimal delivery route to attain the highest tumor uptake of BPA and the tumor-to-normal tissues ratios.

Effect of Anesthesia on Biodistribution of ^{10}B-BPA

The boron concentrations in tumor, ipsilateral brain, contralateral brain, and blood at 2.5 h after administration of 500 mg/kg of BW of BPA under different anesthesia conditions are shown in Figure 4. The boron concentrations in tumor and the ipsilateral brain of the isoflurane-anesthetized rats were significantly lower than those of ketamine mixture–anesthetized rats ($P < 0.01$), whereas the boron concentrations in the contralateral brain ($P = 0.11$) and the blood ($P = 0.52$) were similar in the 2 groups.

DISCUSSION

BNCT is a binary system for cancer treatment that was designed to selectively target heavy charged-particle radiation to tumors at the cellular level. To allow more therapeutic agents to diffuse into the brain and intracerebral neoplasms, a procedure that can temporarily open the BBB has been used (*12*). Intracarotid administration of hypertonic mannitol or cereport leads to a reversible and transient opening of the BBB. When the BBB-D method was applied in clinical chemotherapy and also in preclinical BNCT, the efficiency of treatment (*13,14*) and the survival of animals after neutron irradiation increased significantly (*15,16*). However, to our knowledge, the detailed pharmacokinetics after intracarotid injection of BPA with or without BBB-D has not been reported previously. Therefore, we investigated the pharmacokinetics after intravenous and intracarotid injection of ^{18}F-FBPA and BPA with or without BBB-D using noninvasive and invasive methods.

This study showed that the accumulation of radioactivity in tumor was the highest after intracarotid injection of ^{18}F-FBPA with BBB-D than by other delivery routes (Fig. 1A); the time–activity curve showed a biphasic kinetic pattern. The uptake of ^{18}F-FBPA in tumor after intravenous

TABLE 1
Estimated Pharmacokinetic Parameters Derived from Time–Activity Curves of Blood of F98 Glioma-Bearing Fischer 344 Rats After Intracarotid (i.c.) Injection of ^{18}F-FBPA With and Without BBB-D

Parameter	i.c.	i.c. + BBB-D
k_{el} (min^{-1})	0.0071 ± 0.0014	0.0206 ± 0.0018
k_{12} (min^{-1})	0.0160 ± 0.0017	0.0260 ± 0.0016
k_{21} (min^{-1})	0.0061 ± 0.0004	0.0039 ± 0.0003
V_1 (mL)	3.6 ± 0.1	3.1 ± 0.1
k_{12}/k_{21}	2.6 ± 0.2	6.7 ± 0.5

Each point represents mean ± SD of 6 rats.
All P values for comparison of k_{el}, k_{12}, k_{21}, V_1, and k_{12}/k_{21} were <0.01.

TABLE 2
Biodistribution of ^{18}F-FBPA in Tumor (T), Ipsilateral Brain (IB), Contralateral Brain (CB), and Blood (Bd) of F98 Glioma-Bearing Fischer 344 Rats at 0.5, 2.5, and 4.0 Hours after Intracarotid Administration of ^{18}F-FBPA (29.6 MBq/kg of BW) with BBB-D

	Accumulation (%ID/g)				Ratio		
Time (h)	T	IB	CB	Bd	T/IB	T/CB	T/Bd
0.5	3.32 ± 0.92	1.15 ± 0.44	0.87 ± 0.20	1.72 ± 0.15	2.9	3.8	1.9
2.5	2.63 ± 0.72	0.55 ± 0.21	0.46 ± 0.12	0.39 ± 0.08	4.8	5.7	6.7
4.0	1.48 ± 0.25	0.42 ± 0.08	0.24 ± 0.04	0.18 ± 0.06	3.5	5.9	7.9

Each point represents mean ± SD of 4 or 5 rats. Rats were under isoflurane anesthesia.

administration showed a reasonable delay absorption phase. The time to reach the maximum tumor-to-ispilateral brain ratio was 145–165 min (ratio ~ 5.1) after intracarotid injection with BBB-D, 98–112 min (ratio ~ 3.1) after intracarotid injection without BBB-D, and 45–62 min (ratio ~ 2.4) after intravenous injection (Fig. 1B). The pharmacokinetics of ^{18}F-FBPA in F98 glioma-bearing rats derived from dynamic PET images were further supported by biodistribution studies (Table 2), which showed a tumor-to-ipsilateral brain ratio of 4.8 at 2.5 h after intracarotid injection with BBB-D. The time–radioactivity curves of tumor and ipsilateral brain after intracarotid injection of ^{18}F-FBPA with BBB-D (Fig. 1A) were almost equivalent to the time–boron concentration curves of tumor and ipsilateral brain after intracarotid administration of BPA with BBB-D (Fig. 3A). These results indicated that the pharmacokinetics of ^{18}F-FBPA after intracarotid injection with BBB-D were similar to those of BPA. From the biodistribution (Fig. 3; Tables 2 and 3) and PET study (Fig. 1), we have shown that intracarotid injection of ^{18}F-FBPA and BPA with BBB-D not only significantly increased the accumulation of boron drugs in brain tumor—compared with the results after intracarotid injection without BBB-D or intravenous injection—but also largely elevated the tumor-to-brain and tumor-to-blood ratios. The boron concentration in brain tumor (76.6 μg/g) at 2.5 h after intracarotid injection of 500 mg/kg of BW of BPA with BBB-D was 4-fold higher than that after intravenous injection (19.5 μg/g; Table 3). The high boron concentration in brain tumor and high tumor-to-ipsilateral brain ratio (6.3) may afford enough radiation doses to destroy the tumor cells while sparing the normal tissues in BNCT (*1,2*).

In the absence of lethal treatment toxicities, prolongation of a patient's life depends on preventing tumor regrowth; thus, tumor cell survival probability is a key parameter in treatment success (*17*). For BNCT, the main operational factors that dominate the effectiveness are intracellular boron concentration and thermal neutron fluence. Increasing the neutron exposure will increase the nonspecific background dose to the normal tissues and produce no net gain in the therapeutic ratio. Maximizing the delivery of boron to tumor would be the most effective way to optimize BNCT

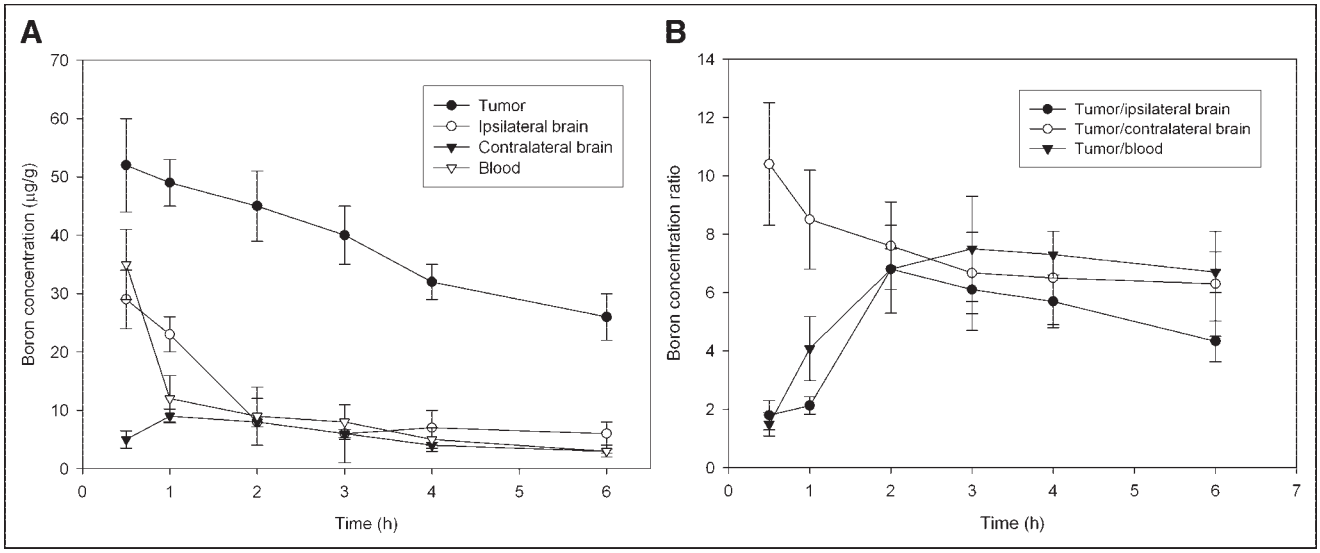

FIGURE 3. Biodistribution of ^{10}B-BPA for F98 glioma-bearing rats. (A) Boron concentration in tumor, ipsilateral brain, contralateral brain, and blood of F98 glioma-bearing Fischer 344 rats after intracarotid injection of BPA (300 mg/kg) with BBB-D. (B) Tumor-to-normal tissue ratio of boron concentration. Rats were under ketamine mixture anesthesia.

TABLE 3
Boron Concentration in Tumor (Tumor [T] Implanted in Left Brain Region), Ipsilateral Brain (IB), Contralateral Brain (CB), and Blood (Bd) of F98 Glioma-Bearing Fischer 344 Rats at 2.5 Hours After Administration of BPA (500 mg/kg) by Various Routes

Route	Boron concentration (μg/g)				Ratio		
	T	IB	CB	Bd	T/IB	T/CB	T/Bd
i.c. + BBB-D	76.6 ± 12.1	12.1 ± 3.5	10.1 ± 1.5	9.2 ± 2.4	6.3	7.6	8.3
i.c.	43.1 ± 5.6	10.5 ± 0.9	9.3 ± 0.2	9.5 ± 1.4	4.1	4.6	4.5
i.v.	19.5 ± 4.5	7.8 ± 1.4	8.4 ± 1.6	9.0 ± 1.2	2.5	2.3	2.2

i.c. = intracarotid; i.v. = intravenous.
Each point represents mean ± SD of 5 or 6 rats. Rats were under ketamine mixture anesthesia.

(*2*). The results of this study indicated that intracarotid injection of BPA with BBB-D, compared with other delivery routes such as intravenous or intracarotid, builds the highest boron concentration in tumor and, thus, may exhibit a dramatic effect on the therapeutic efficacy. The most common delivery route of boron drugs in clinical BNCT to date is intravenous administration. The patients in past BNCT studies have not shown a significant benefit from BNCT treatment (*18,19*), perhaps partially because of the insufficient boron content and boron-to-normal tissue ratio to reach a tumor curative radiation dose by intravenous administration of boron-containing drugs.

Lower tumor-to-ipsilateral brain and tumor-to-blood ratios derived from ^{18}F radioactivity measurement (Fig. 1B; Table 2) than those obtained from boron concentration determination (Fig. 3B; Table 3) were repeatedly observed in this study. To address this issue, a study was performed to clarify whether this phenomenon was caused by the different elements determined. A mixture of ^{18}F-FBPA (29.6 MBq/kg of BW) and BPA (300 mg/kg of BW) was administered into the glioma-bearing rats by intracarotid injection with BBB-D. The ^{18}F radioactivity in the tumor and tissue samples was measured with a γ-scintillation counter, and the boron content in the samples was determined with ICP-MS at 24 h after ^{18}F radioactivity measurement. The tumor-to-ipsilateral brain, tumor-to-contralateral brain, and tumor-to-blood ratios obtained from boron concentration determination were 7.2, 8.1, and 8.3, respectively, and those obtained from ^{18}F radioactivity measurement were 7.6, 8.3, and 8.9, respectively, at 2.5 h after drug administration (Table 4). Agreement between the ratios eliminated our doubt and revealed the same biodistribution of ^{18}F-FBPA and BPA after intracarotid administration with BBB-D, which is similar to our previous study that showed the biodistribution of ^{18}F-FBPA was consistent with that of BPA after intravenous administration (*7*).

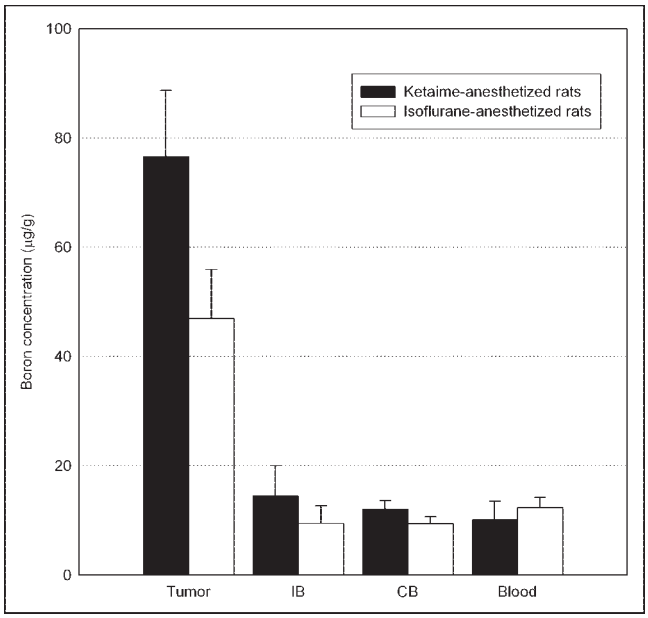

FIGURE 4. Boron concentration in tumor, ipsilateral brain (IB), contralateral brain (CB), and blood at 2.5 h after administration of 500 mg/kg of BW of BPA under isoflurane/ketamine mixture anesthesia.

To further elucidate the differences observed in Tables 2 and 3, another study using intracarotid injection of BPA into the BBB-disrupted glioma-bearing rats, but anesthetized with different agents, was performed. The results (Fig. 4) showed that the boron concentrations of the contralateral brain and blood under different anesthetic conditions were similar, whereas the boron concentrations of tumor and ipsilateral brain in the isoflurane-anesthetized rats were lower than those in the ketamine mixture–anesthetized rats. Our results indicated that the degree of the BBB-D induced by mannitol infusion was less in glioma-bearing rats under isoflurane anesthesia than that under ketamine mixture anesthesia. It has been suggested that the degree of hyperosmolar BBB-D depends on the anesthetic conditions and the anesthetic agents used (*20–22*). Isoflurane, fentanyl, and pentobarbital anesthesia decreased the basal permeability of the BBB when compared with the awake condition. Chi et al. (*23*) have demonstrated that the degree of BBB-D induced by hyperosmolar mannitol was less under isoflurane anesthesia than that under pentobarbital anesthesia.

The pharmacokinetics derived from the open 2-compartment model after intravenous injection of BPA and BSH in

TABLE 4
Biodistribution of ^{18}F-FBPA and BPA in Tumor (T), Ipsilateral Brain (IB), Contralateral Brain (CB), and Blood (Bd) of F98 Glioma-Bearing Fischer 344 Rats at 2.5 Hours After Intracarotid Injection of a Mixture of ^{18}F-FBPA (29.6 MBq/kg) and BPA (300 mg/kg) with BBB-D

	Accumulation				Ratio		
Element	T	IB	CB	Bd	T/IB	T/CB	T/Bd
^{18}F (%ID/g)	4.63 ± 0.72	0.61 ± 0.08	0.56 ± 0.12	0.52 ± 0.08	7.6	8.3	8.9
^{10}B (μg/g)	45.5 ± 3.4	6.3 ± 0.23	5.6 ± 0.12	5.5 ± 0.33	7.2	8.1	8.3

Each point represents mean ± SD of 3 rats. Rats were under ketamine mixture anesthesia.

clinical BNCT have been reported (*24–26*). Some investigators have proposed modified 3-compartment models to describe the observed pharmacokinetics in brain after intravenous injection of ^{18}F-FBPA in clinical and animal applications (*27,28*). In this study, the time–activity curves of blood obtained after intracarotid injection of ^{18}F-FBPA with and without BBB-D (Fig. 2) were both biexponential, but with different slopes in the elimination phase during the study period. Thus, the open 2-compartment model was used to estimate the pharmacokinetic parameters. The higher value of k_{12} in the intracarotid group with BBB-D than that in the intracarotid group without BBB-D (Table 1) indicated that ^{18}F-FBPA was transported from blood into the brain more readily through the hyperosmotically disrupted BBB. In addition to BBB-D, mannitol has been reported to increase the glomerular filtration rate and renal blood flow (*29*). Our previous study (*7*) showed that renal clearance is the major metabolism route of ^{18}F-FBPA and, thus, the elimination of ^{18}F-FBPA (k_{el}; Table 1) from the blood in the intracarotid group with BBB-D should be faster than that in the intracarotid group without BBB-D, which was also observed in this study. Elevation of the boron concentration in the brain tumor after intracarotid injection of boron compounds was highly dependent on the extent of BBB-D; therefore, it is critical to assess the extent of BBB-D for each individual patient before neutron irradiation is conducted. The k_{12}/k_{21} ratio, which is linearly correlated with the accumulation of ^{18}F-FBPA in tumor (r^2 = 0.915; Fig. 5A), and the tumor-to-ipsilateral brain ratio (r^2 = 0.941; Fig. 5B) may render a direct indication of BBB-D and provide the information needed for actual dosage adjustment to achieve optimal BNCT.

CONCLUSION

This study demonstrated that the boron concentration in tumor and the tumor-to-normal brain ratio after intracarotid injection of BPA with BBB-D are significantly higher than

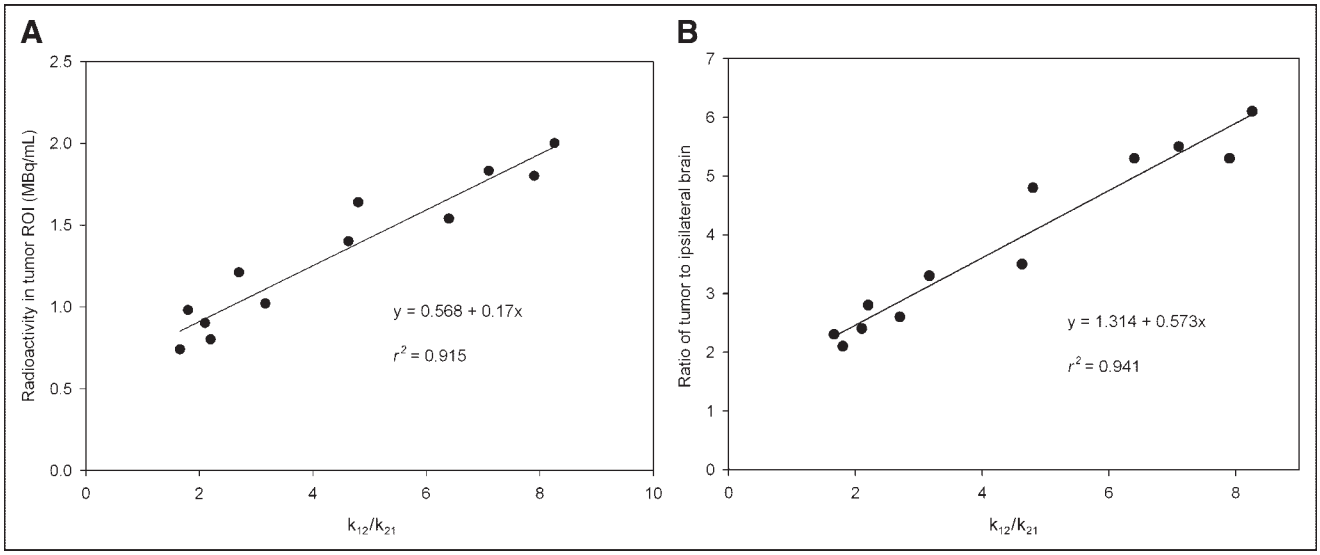

FIGURE 5. Correlation among tumor region of interest (ROI), k_{12}/k_{21}, and tumor-to-ipsilateral brain ratio. (A) Correlation between radioactivity of tumor ROI and k_{12}/k_{21}. (B) Correlation between tumor-to-ipsilateral brain ratio and k_{12}/k_{21}. Each point represents one rat. Radioactivity of tumor ROI and tumor-to-ipsilateral brain ratio were derived from PET images at 2.5 h after intracarotid injection of ^{18}F-FBPA with and without BBB-D. k_{12}/k_{21} ratio was obtained from pharmacokinetic analysis of blood of the same rat.

that by other delivery routes. The biodistributions of ^{18}F-FBPA and BPA after intracarotid administration with BBB-D in glioma-bearing rats were almost equivalent; thus, an ^{18}F-FBPA PET scan may reveal the pharmacokinetics of BPA after intracarotid injection with BBB-D and suggest the optimal window for effective BNCT. The BBB-D induced by intracarotid injection of hyperosmolar mannitol could vary depending on anesthetic agents and anesthetic conditions and should be considered in the design of treatment protocols of BNCT. The k_{12}/k_{21} ratio offered a good indication of the extent of BBB-D and could be used to evaluate the boron concentration in the tumor and tumor-to-brain ratio after intracarotid injection of BPA with BBB-D in the future clinical BNCT application.

ACKNOWLEDGMENTS

This study was supported by grants NSC89-2745-P-010-003, NSC91-2745-P-010-001, NSC92-2745-P-010-002, and 92 GMP 005 from the National Science Council, Taipei, Taiwan. We thank the staff of the national PET and Cyclotron Center in Taipei Veterans General Hospital, who provided the radiopharmaceuticals and other assistance. We also thank the staff of the Instrumentation Center at the National Tsing Hua University, Hsinchu, Taiwan, for the technical support in performing the boron assay.

REFERENCES

1. Fairchild RG, Bond VP. Current status of ^{10}B-neutron capture therapy: enhancement of tumor dose via beam filtration and dose rate, and the effects of these parameters on minimum boron content: a theoretical evaluation. *Int J Radiat Oncol Biol Phys.* 1985;11:831–840.
2. Coderre JA, Morris GM. The radiation biology of boron neutron capture therapy. *Radiat Res.* 1999;151:1–18.
3. Hatanaka H, Nakagawa Y. Clinical results of long-surviving brain tumor patients who underwent boron neutron capture therapy. *Int J Radiat Oncol Biol Phys.* 1994;28:1061–1066.
4. Kato I, Ono K, Sakurai Y, et al. Effectiveness of BNCT for recurrent head and neck malignancies. *Appl Radiat Isot.* 2004;61:1069–1073.
5. Barth RF, Yang W, Bartus RT, et al. Neutron capture therapy of intracerebral melanoma: enhanced survival and cure after blood-brain barrier opening to improve delivery of boronophenylalanine. *Int J Radiat Oncol Biol Phys.* 2002; 52:858–868.
6. Barth RF, Yang W, Rotaru JH, et al. Boron neutron capture therapy of brain tumors: enhanced survival following intracarotid injection of either sodium borocaptate or boronophenylalanine with or without blood-brain barrier disruption. *Cancer Res.* 1997;57:1129–1136.
7. Wang HE, Wu SY, Chang CW, et al. Evaluation of 4-borono-2-^{18}F-fluoro-L-phenylalanine-fructose as a probe for boron neutron capture therapy in a glioma-bearing rat model. *J Nucl Med.* 2004;45:302–308.
8. Neuwelt EA, Minna J, Frenkel E, Barnett PA, McCormick CI. Osmotic blood-brain barrier opening to IgM monoclonal antibody in the rat. *Am J Physiol.* 1986;250:875–883.
9. Neuwelt EA, Barranger JA, Pagel MA, Quirk JM, Brady RO, Frenkel EP. Delivery of active hexosaminidase across the blood-brain barrier in rats. *Neurology.* 1984;34:1012–1019.
10. Cosolo WC, Martinello P, Louis WJ, Christophidis N. Blood-brain barrier disruption using mannitol: time course and electron microscopy studies. *Am J Physiol.* 1989;256:443–447.
11. Sah RN, Brown PH. Boron determination: a review of analytical methods. *Microchem J.* 1997;56:285–304.
12. Kroll RA, Neuwelt EA. Outwitting the blood-brain barrier for therapeutic purposes: osmotic opening and other means. *Neurosurgery.* 1998;42:1083–1099.
13. Neuwelt EA, Goldman DL, Dahlborg SA, et al. Primary CNS lymphoma treated with osmotic blood-brain barrier disruption: prolonged survival and preservation of cognitive function. *J Clin Oncol.* 1991;9:1580–1590.
14. Gumerlock MK, Belshe BD, Madsen R, Watts C. Osmotic blood-brain barrier disruption and chemotherapy in the treatment of high grade malignant glioma: patient series and literature review. *J Neurooncol.* 1992;12:33–46.
15. Yang W, Barth RF, Rotaru JH, et al. Enhanced survival of glioma bearing rats following boron neutron capture therapy with blood-brain barrier disruption and intracarotid injection of boronophenylalanine. *J Neurooncol.* 1997;33:59–70.
16. Yang W, Barth RF, Rotaru JH, et al. Boron neutron capture therapy of brain tumors: enhanced survival following intracarotid injection of sodium borocaptate with or without blood-brain barrier disruption. *Int J Radiat Oncol Biol Phys.* 1997;37:663–672.
17. Steel GG. *Basic Clinical Radiobiology*. 2nd ed. New York, NY: Oxford University Press, Inc.; 2000.
18. Nakagawa Y, Hatanaka H. Boron neutron capture therapy: clinical brain tumor studies. *J Neurooncol.* 1997;33:105–115.
19. Joensuu H, Kankaanranta L, Seppala T, Auterinen I, Kallio M, Kulvik M. Boron neutron capture therapy of brain tumors: clinical trials at the Finnish facility using boronophenylalanine. *J Neurooncol.* 2003;61:123–134.
20. Chi OZ, Wei HM, Anwar M, Sinha AK, Klein SL, Weiss HR. Effects of fentanyl on alpha-aminoisobutyric acid transfer across the blood-brain barrier. *Anesth Analg.* 1992;75:31–36.
21. Chi OZ, Anwar M, Sinha A, Wei HM, Klein SL, Weiss HR. Effects of isoflurane on transport across the blood-brain barrier. *Anesthesiology.* 1992;76:426–431.
22. Saija A, Princi P, De Pasquale R, Costa G. Modifications of the permeability of the blood-brain barrier and local cerebral metabolism in pentobarbital- and ketamine-anaesthetized rats. *Neuropharmacology.* 1989;28:997–1002.
23. Chi OZ, Chun TW, Liu X, Weiss HR. The effects of pentobarbital on blood-brain barrier disruption caused by intracarotid injection of hyperosmolar mannitol in rats. *Anesth Analg.* 1998;86:1230–1235.
24. Kageji T, Nagahiro S, Kitamura K, et al. Optimal timing of neutron irradiation for boron neutron capture therapy after intravenous infusion of sodium borocaptate in patients with glioblastoma. *Int J Radiat Oncol Biol Phys.* 2001;51:120–130.
25. Kiger WS 3rd, Palmer MR, Riley KJ, Zamenhof RG, Busse PM. Pharamacokinetic modeling for boronophenylalanine-fructose mediated neutron capture therapy: ^{10}B concentration predictions and dosimetric consequences. *J Neurooncol.* 2003;62:171–186.
26. Kiger WS 3rd, Palmer MR, Riley KJ, Zamenhof RG, Busse PM. A pharmacokinetic model for the concentration of ^{10}B in blood after boronophenylalanine-fructose administration in humans. *Radiat Res.* 2001;155:611–618.
27. Chen JC, Chang SM, Hsu FY, Wang HE, Liu RS. MicroPET-based pharmacokinetic analysis of the radiolabeled boron compound [^{18}F]FBPA-F in rats with F98 glioma. *Appl Radiat Isot.* 2004;61:887–891.
28. Imahori Y, Ueda S, Ohmori Y, et al. Fluorine-18-labeled fluoroboronophenylalanine PET in patients with glioma. *J Nucl Med.* 1998;39:325–333.
29. Behnia R, Koushanpour E, Brunner EA. Effects of hyperosmotic mannitol infusion on hemodynamics of dog kidney. *Anesth Analg.* 1996;82:902–908.